Supporting Information

Sherwood et al. 10.1073/pnas.1016709108

SI Materials and Methods

MRI Acquisition. *Chimpanzees.* For in vivo scans, subjects were first immobilized by ketamine (10 mg/kg) or telazol (3–5 mg/kg) and subsequently anesthetized with propofol (40–60 mg·kg·h) following standard procedures at the Yerkes National Primate Research Center (YNPRC). Subjects were then transported to the MRI facility. The subjects remained anesthetized for the duration of the scans as well as the time needed to transport them between their home cage and the imaging facility (total time ~1.5 h). Subjects were placed in the scanner chamber in a supine position with their head fitted inside the human-head coil. Scan duration ranged between 30 and 40 min as a function of brain size. The chimpanzees were scanned using either a 1.5 T or a 3 T scanner (Siemens Trio, Siemens Medical Solutions) at the YNPRC. For all chimpanzees scanned in vivo using the 1.5 T machine (Phillips Model 51), T1-weighted images were collected in the transverse plane using a gradient echo protocol [pulse repetition (TR) = 19.0 ms, echo time (TE) = 8.5 ms, number of signals averaged = 8, and a 256 × 256 matrix]. For the apes scanned in vivo at 3 T (Siemens Trio), T1-weighted images were collected using a 3D gradient-echo sequence (TR = 2,300 ms; TE = 4.4 ms; number of signals averaged = 3; matrix size = 320 × 320, with 0.6 × 0.6 × 0.6 resolution). After completing MRI procedures, the chimpanzee subjects were returned to the YNPRC and temporarily housed in a single cage for 6 to 12 h to allow the effects of the anesthesia to wear off, after which they were returned to their home cage. Postmortem chimpanzee brains were scanned using the same protocol described above with a 3 T scanner.

Humans. Thin-cut T1-weighted MR images were obtained in vivo in the human subjects using a GE Signa scanner operating at 1.5 T and the following protocol: SPGR/50, TR = 24 ms, TE = 7 ms, NEX = 1, matrix size of 256 × 192, and FOV = 24 cm. We obtained 124 contiguous coronal slices, 1.5- or 1.6-mm thick and interpixel distance of 0.94 mm. The slice thickness was adjusted to the size of the brain so as to sample the entire brain but avoid wrap artifacts. Three individual datasets were obtained for each brain during each imaging session. These datasets were coregistered and averaged post hoc using automated image registration (AIR 3.03, University of California at Los Angeles), to produce a single dataset of enhanced quality with pixel dimensions of 0.7 mm in plane and interslice spacing of 1.5 mm between planes.

Volumetric Measurements. All human brains were reconstructed in three dimensions using Brainvox (1), an interactive family of programs designed to reconstruct, segment, and measure brains from MR-acquired images. Images of chimpanzee brain were reconstructed in Analyze 7.0 software (Mayo Clinic, Mayo Foundation, Rochester, MN). For humans, an in-house automated program, extensively validated against human experts (2), was used to segment the images into the three primary tissue types (white, gray, cerebrospinal fluid). Similarly, in chimpanzees, FSL software (Analysis Group, Functional MRI of the Brain, Oxford, United Kingdom) was used to segment images into cerebrospinal fluid, gray and white matter. ROI were traced by hand on contiguous coronal slices of the realigned brains.

ROIs were segmented according to protocols that have been previously described (3–5). In brief, total neocortical gray-matter volume measurements were made from coronal sections and included the entire cortical mantle, excluding tissue located mesial to the rhinal sulcus. According to these criteria, our definition of neocortical gray matter included proisocortex (cingulate gyrus, rostral insula, and temporal pole) but did not include the hippocampus. Measurement of the total neocortical white-matter volume included the corpus callosum and the cingulum bundle, but excluded the white matter underlying the hippocampus. In chimpanzees the white-matter volume excluded the internal and external capsules; in humans these structures were included. Measurements of frontal lobe gray and white matter were performed on coronal sections and were bounded by the lateral sulcus and the central sulcus. Anatomical landmarks were identified and marked on the surface of 3D reconstructions. In sections including the central sulcus, only gray and white matter located mesial and superior to the central sulcus was measured. The hippocampal formation, including the dentate gyrus, hippocampus proper, and subiculum was measured as a single structure. The mesial boundary of the hippocampus was defined where the subiculum transitions into the parahippocampal gyrus. Although the ROIs were traced separately in each hemisphere, initial analysis did not reveal asymmetry in these measures, therefore the volumes of the two hemispheres were combined. Fig. S5 shows examples of MRI scans.

Power Analysis. The statistical significance of age as an independent variable upon which brain-region size is dependent was evaluated by using an *F*-test to compare a regression model, which includes all variables except age (sex in humans, and sex and scan type in chimpanzees) to a regression model, which includes the age terms. The effect size associated with this comparison can be expressed in terms of the sum of squared error (residuals) from each of the two models:

$$(SSE_1 - SSE_2)/SSE_1$$

where SSE_1 is the sum of squared error for the model without an age effects, and SSE_2 corresponds to the model including age. Similar to the coefficient of determination, a value of 1 indicates that the model that includes age effects fits the data perfectly, whereas a value of 0 indicates that the inclusion of age does not improve the model fit at all.

In the absence of information regarding age-related changes in brain-region size in chimpanzees, there is no a priori expectation of a meaningful proportional reduction in model error because of the inclusion of age. Instead, the power analysis uses the effect size found in a given human model (e.g., 0.231 for the cubic model fit to neocortical gray matter volume) and uses the *F*-distribution to determine the required sample size required to find that effect size as significant at $\alpha = 0.05$ in the corresponding chimpanzee sample, taking into account the differences in number of variables.

For each model, significance of the age effect was originally calculated as described above. Then the oldest individual (or individuals if two or more members of the sample were the same age in years) was removed from the sample and the significance of the age terms was recalculated. This procedure was repeated until the age effect was no longer significant at $\alpha = 0.05$. *P* values were calculated in two ways: (*i*) using the reduced degrees of freedom reflecting the smaller sample size from the removal of the oldest individuals in the sample, and (*ii*) using the full degrees of freedom found in the original sample size, which prevents models from being found nonsignificant simply because of smaller sample size. The two methods produced similar results (Table 3). All analyses were conducted using the statistical programming environment *R*, version 2.10.0 (R Development Core Team 2009).

1. Frank RJ, Damasio H, Grabowski TJ (1997) Brainvox: An interactive, multimodal visualization and analysis system for neuroanatomical imaging. *Neuroimage* 5(1): 13–30.
2. Grabowski TJ, Frank RJ, Szumski NR, Brown CK, Damasio H (2000) Validation of partial tissue segmentation of single-channel magnetic resonance images of the brain. *Neuroimage* 12:640–656.
3. Allen JS, Bruss J, Brown CK, Damasio H (2005) Normal neuroanatomical variation due to age: The major lobes and a parcellation of the temporal region. *Neurobiol Aging* 26: 1245–1260, discussion 1279–1282.
4. Sherwood CC, et al. (2004) Brain structure variation in great apes, with attention to the mountain gorilla (*Gorilla beringei beringei*). *Am J Primatol* 63(3):149–164.
5. Semendeferi K, Damasio H, Frank R, Van Hoesen GW (1997) The evolution of the frontal lobes: A volumetric analysis based on three-dimensional reconstructions of magnetic resonance scans of human and ape brains. *J Hum Evol* 32: 375–388.

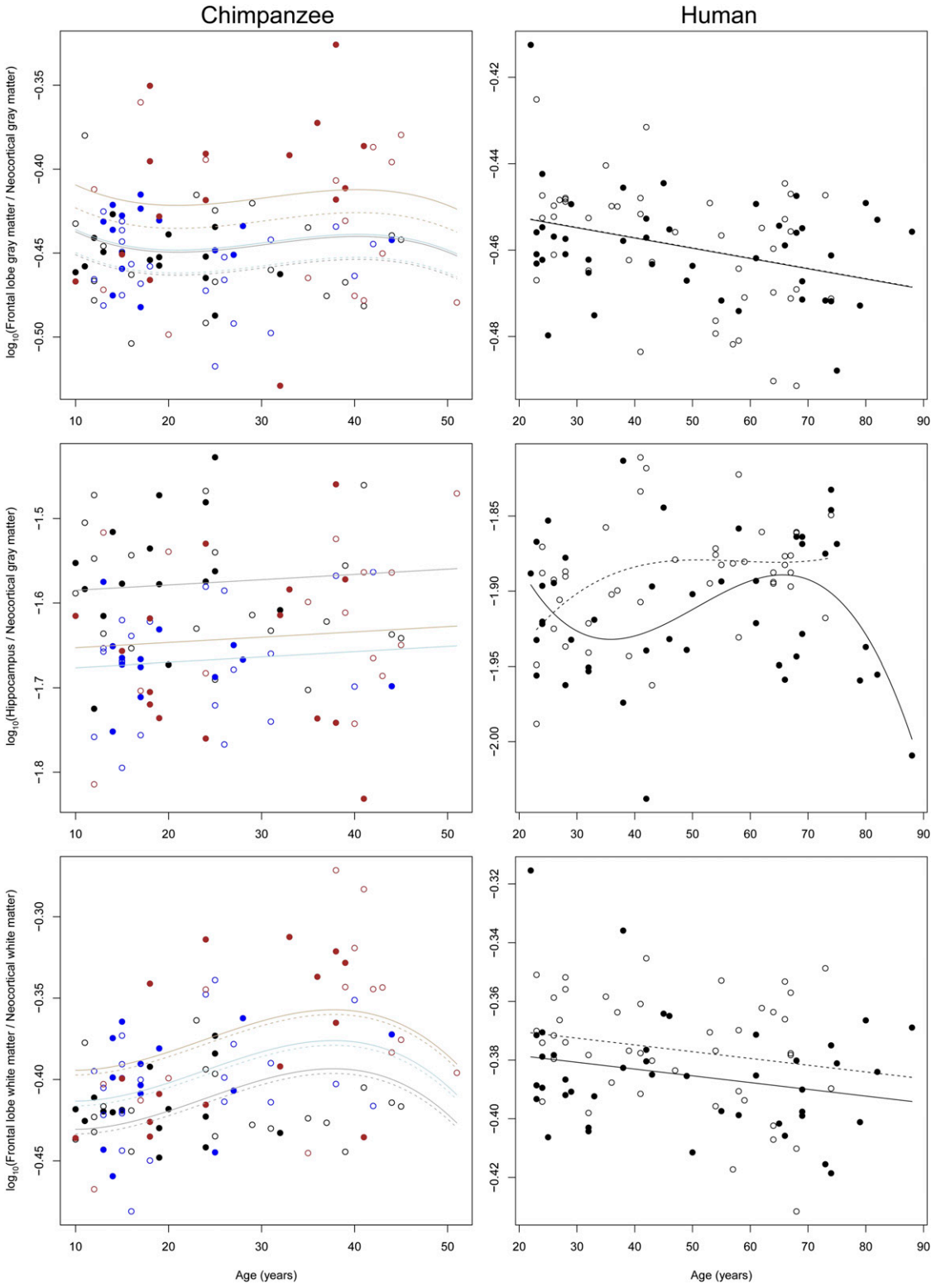

Fig. S1. Relative brain-region volume versus age in chimpanzees and humans. Open symbols are females, closed symbols are males. For humans, the solid line indicates the best-fit curve superimposed on males and the dashed line indicates the best-fit curve superimposed on females. Note that separate cubic models have been fit to males and females for human relative hippocampus size (Table 2). For chimpanzees, curves represent model fits with the lowest *P* values, but none are significant at $\alpha = 0.05$ (Table 1). For chimpanzees, blue datapoints are individuals scanned at 3 T, black datapoints are individuals scanned at 1.5 T; brown datapoints represent postmortem 3 T scans. Colored lines correspond to datapoints of the same color. The chimpanzee curves are not significant at $\alpha = 0.05$, with the exception of relative frontal lobe white-matter size (Table 2).

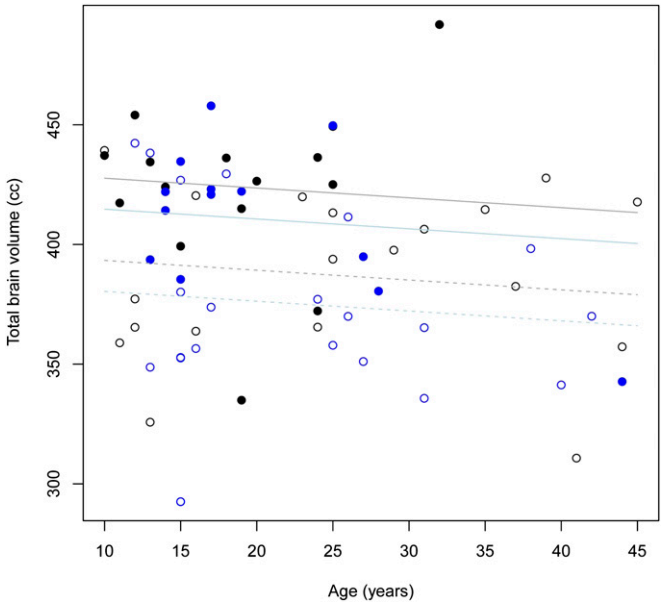

Fig. S2. Total brain volume versus age in chimpanzees. Open symbols are females, closed symbols are males. Blue datapoints are individuals scanned at 3 T, all other individuals scanned at 1.5 T. Solid lines correspond to male trends, dashed lines to female trends, and colors correspond to data point colors. Trend lines represent model fits with lowest *P* values, but none are significant at $\alpha = 0.05$ (Table 1).

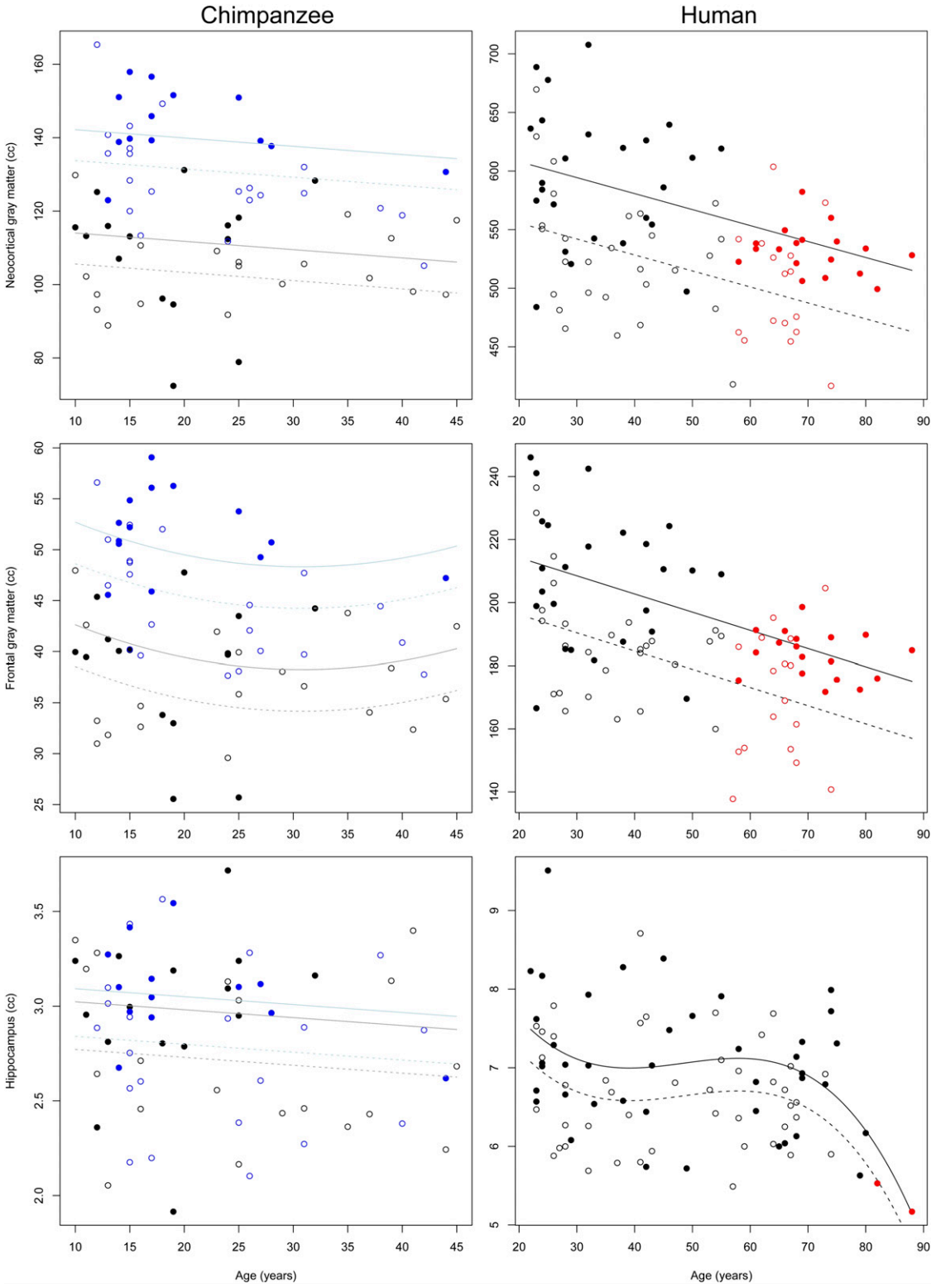

Fig. S3. Gray-matter regions of interest versus age in chimpanzees and humans. Open symbols are females, closed symbols are males. For humans, the solid line indicates the best-fit curve superimposed on males, dashed line indicates the best-fit curve superimposed on females. For chimpanzees, curves represent model fits with the lowest *P* values, but none are significant at $\alpha = 0.05$ (Table 1). Blue datapoints are individuals scanned at 3 T, all other individuals scanned at 1.5 T; colored lines correspond to datapoints of same color. Red datapoints are those human individuals, which are at the cutoff age or older (Table 3).

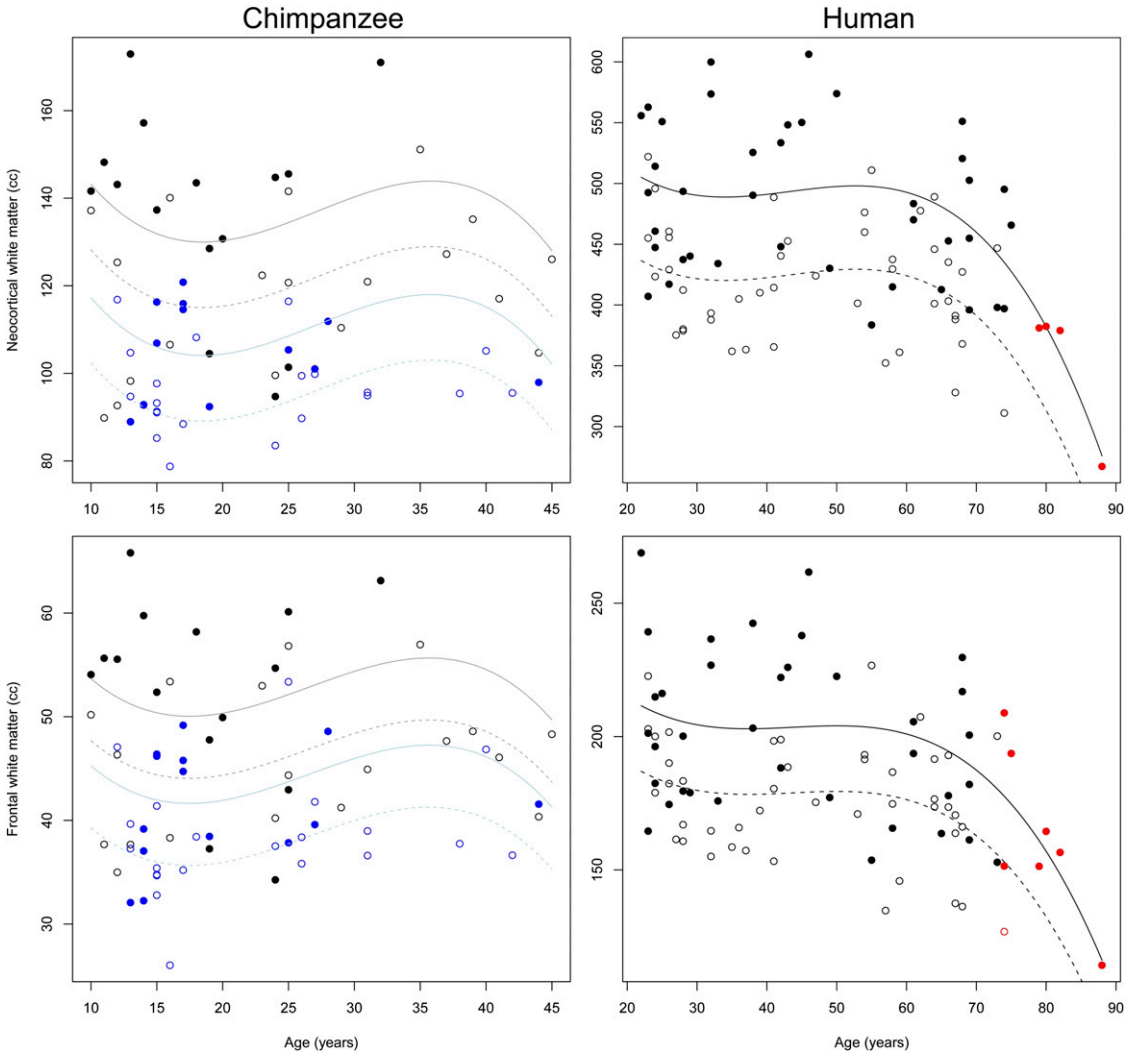

Fig. S4. White-matter regions of interest versus age in chimpanzees and humans. Symbols and lines follow Fig. S3. For chimpanzees, curves represent model fits with the lowest *P* values, but none are significant at $\alpha = 0.05$ (Table 1).

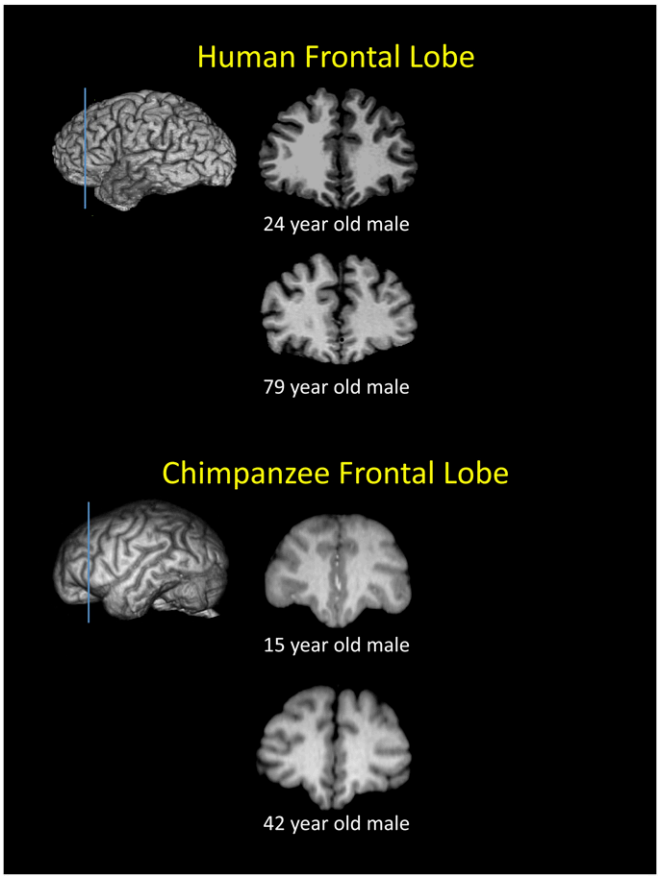

Fig. S5. Coronal MRI sections through the frontal lobes of adult humans and chimpanzees of various ages.

Other Supporting Information Files

Dataset S1 (XLS)